Effects of the Blend Ratio and Crosslinking Systems on the Curing Behavior, Morphology, and Mechanical Properties of Styrene–Butadiene Rubber/Poly(ethylene-*co*-vinyl acetate) Blends

C. K. Radhakrishnan,[1] A. Sujith,[1] G. Unnikrishnan,[1] Sabu Thomas[2]

[1]*National Institute of Technology, Calicut 673601, Kerala, India*
[2]*School of Chemical Sciences, Mahatma Gandhi University, Kottayam 686560, Kerala, India*

Received 29 August 2003; accepted 6 May 2004
DOI 10.1002/app.20939
Published online in Wiley InterScience (www.interscience.wiley.com).

ABSTRACT: Blends of styrene–butadiene rubber (SBR) and poly(ethylene-*co*-vinyl acetate) (EVA) with different ratios were prepared with a two-roll mixing mill and were vulcanized by three different crosslinking systems, namely, sulfur (S), dicumyl peroxide, and a mixture consisting of S and peroxide (mixed). The vulcanization behavior of the blends was analyzed from the rheographs. The mechanical properties, including stress–strain behavior, tensile strength, elongation at break, modulus, hardness, and abrasion resistance, of the blends were examined. The morphology of the prepared blends was studied with scanning electron microscopy with special reference to the effects of the blend ratio and crosslinking systems. A relatively cocontinuous morphology was observed for the 20/80 SBR/EVA composition. The mechanical properties increased with increasing EVA content up to 60–80%, for all of the vulcanizing modes. The tensile fracture surfaces were analyzed under a scanning electron microscope to understand the failure mechanism. Various theoretical models were applied to explain the properties of the blends. © 2004 Wiley Periodicals, Inc. J Appl Polym Sci 94: 827–837, 2004

Key words: blends; morphology; vulcanization; mechanical properties

INTRODUCTION

The aim of polymer blending is to develop products with unique properties that cannot be attained from individual components. The performance of a polymer blend is determined by various factors, including the nature of the individual components, type of vulcanizing agent, processing parameters, and to a certain extent, the application for which it is intended. Polymer blends have attracted more interest because new molecules are not always required for the preparation of materials with new macroscopic properties and because blending is more rapid and economical than the development of a new polymer.

Since the rapid growth of commercial polymer blends in the 1980s, extensive studies have been done on them.[1–5] Interesting studies on blends of styrene–butadiene rubber (SBR) and poly(ethylene-*co*-vinyl acetate) (EVA) with other elastomers exist in the literature. For example, Nelson and Kutty[6] studied the cure characteristics and mechanical properties of maleic anhydride-grafted-whole tire reclaim and SBR blends. They found that the mechanical properties of the blends containing grafted whole tire reclaim were better than those of the unmodified blends. Amraee et al.[7] proposed a new method to analyze SBR/polybutadiene rubber blends in passenger tire tread compounds by thermogravimetric analysis. Ismail and Suzaimah[8] studied the dynamic properties, curing characteristics, and swelling behavior of SBR and epoxidized natural rubber (ENR) blends. They observed that the incorporation of ENR 50 in the blends improved the processability, stiffness, and resilience and reduced the damping properties. The influence of blend composition on the internal friction of natural rubber (NR) and SBR compounds was studied by Ghilarducci et al.[9] Mechanical dynamic measurements were used in that study to analyze the behavior of cured, carbon-black-filled NR/SBR blends with a sulfur (S)/accelerator system. They noticed a secondary transition appearing at temperatures between 100 and 160 K in addition to glass transition.

Varghese et al.[10] studied the effects of blend ratio, crosslinking systems, and fillers on the morphology, curing behavior, mechanical properties, and failure mode of acrylonitrile butadiene rubber (NBR) and EVA blends. They used three different crosslinking systems, namely, S, dicumyl peroxide (DCP), and a

Correspondence to: G. Unnikrishnan (unnig@nitc.ac.in).
Contract grant sponsor: Council of Scientific and Industrial Research, New Delhi, India (support to G.U.).

TABLE I
Details of The Materials

Material	Characteristics		Source
SBR-1502	Styrene content (%)	24.00	
	Volatile matter (%)	0.75	
	Organic acid	4.75	Korea Kumho
	Soap	0.50	Petrochemicals
	Ash	1.50	
	Antioxidant	0.50	
	Density (g/cc)	0.94	
	Mooney viscosity (ML_{1+4}, 100°C)	46.00	
EVA-1802	Melt flow index (g/10 min)	2.00	
	Density (g/cc)	0.94	National Organic and Chemical Industries
	Vicat softening point (°C)	59.00	
	Vinyl acetate (%)	18.00	
	Intrinsic viscosity (dLg)	0.17	

mixed system (S+DCP) and found that the mixed system exhibited better mechanical properties than the other systems. The effect of the blend ratio on the crosslinking characteristics of EVA and ethylene–propylene–diene tercopolymer (EPDM) blends was studied by Mishra et al.[11] by differential scanning calorimetry and torque rheometry. The results showed that the cure rate (RH) increased, whereas the optimum cure time and energy consumption for curing decreased with increasing EVA/EPDM blend ratio. Yoon et al.[12] studied the thermal and mechanical properties of poly(L-lactic acid) (PLLA) and EVA blends and reported that the tensile strength and modulus of the PLLA/EVA blends dropped rapidly, followed by a more gradual decrease, with increasing EVA content. Blends of EVA with unsaturated rubbers such as polychloroprene[13,14] and NR[15,16] have also been developed. SBR/EVA blends have been reported to produce thermoplastic moldable shoe sole material by dynamic vulcanization.[17]

SBR is a general purpose, multiuse synthetic rubber with a high filler loading capacity and good flex resistance, crack-initial resistance, and abrasion resistance, which make it useful for several engineering and industrial applications. However, as with other unsaturated rubbers, it has poor aging characteristics. To minimize the oxidative degradation of SBR during service at high temperatures, it is important to blend it with a saturated or low unsaturated polymer. EVA may be considered a good partner for this purpose because it offers excellent aging resistance, weather resistance, toughness, chemical resistance, and processability. The objective of this study was to examine the effects of the blend ratio and crosslinking systems on the curing behavior, morphology, and mechanical properties of SBR/EVA blends. DCP was used for crosslinking both SBR and EVA. S was used as another crosslinking system for this blend system. However, S could crosslink only the SBR phase and not EVA because of the saturated backbone structure of the latter. Hence, a mixed system containing both peroxide and S was also selected for the effective curing of both of the phases in the blends.

EXPERIMENTAL

Materials

SBR, marketed under the trade name Syanaprene (SBR-1502), was obtained from Korea Kumho Petrochemical Co., Ltd. (Ulsan, Korea). The EVA used was EVA-1802 obtained from National Organic and Chemical Industries, Ltd. (Mumbai, India). The basic characteristics of SBR and EVA are given in Table I. The rubber chemicals used, including S, DCP, zinc oxide, stearic acid, and mercaptobenzothiazyl disulfide (MBTS), were commercial grade.

Blend preparation

Blends of SBR and EVA with different blend ratios and crosslinking systems were prepared on a two-roll mixing mill with a friction ratio of 1:1.4. The compounding recipes of the blends are given in Table II. The different crosslinking systems used, namely, S, DCP, and S+DCP, are indicated as S, P, and M, re-

TABLE II
Formulation of the Mixes (phr)

Ingredient (phr)	Sulfur system	Peroxide system	Mixed system
Polymer	100	100	100
Zinc oxide	4	—	4
Stearic acid	2	—	2
MBTS	1.5	—	1.5
Sulfur	2	—	2
DCP	—	4	4

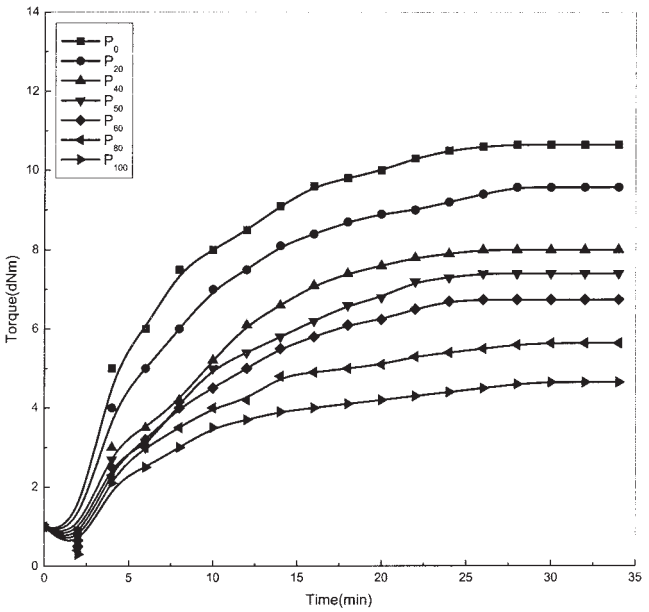

Figure 1 Rheographs of the DCP-cured SBR/EVA blends.

spectively. The compounds containing the S system are designated as S_0 (pure SBR), S_{20} (80/20 SBR/EVA), S_{40} (60/40 SBR/EVA), and so on. Similarly, the compounds containing peroxide and the mixed cured systems are designated, respectively, as P_0 and M_0 (pure SBR), P_{20} and M_{20} (80/20 SBR/EVA), P_{40} and M_{40} (60/40 SBR/EVA), and so on. The subscripts indicate the weight percentage of EVA in the blends. The cure characteristics of the blends were studied with a Monsanto moving disc rheometer (MDR 2000, Akron, OH, USA). The compounded blends were then compression-molded with a hydraulic press for tensile and hardness sheets at 160°C under a pressure of 30 tons for optimum curing. The S_{100} and M_{100} samples could not be molded, probably because the backbone of EVA was saturated. The samples for tensile and tear tests were punched along the mill direction from the molded tensile sheets. Samples for abrasion resistance were punched from hardness sheets 6 mm thick.

Mechanical properties

The test samples were dried at 60°C for 3 h to remove moisture. Tensile testing of the samples was done at 25 ± 2°C according to the ASTM D 412 test method with dumbbell-shaped test specimens at a crosshead speed of 500 mm/min with the Series IX Automated Material Testing System 1.38 by Instron Corp. model 441 (Canton, MA, USA). The tear strength was examined as per ASTM D 624 with 90° angle test pieces. The experimental conditions of temperature and crosshead speed for the tear measurements were also the same as that of the tensile testing. The hardness of the samples was measured as per ASTM D 2240 with a Mitutoyo Shore A meter (Japan). For this measurement, sheets with an effective thickness of 6 mm were used. The relative volume loss was measured with a Zwick-made Deutsches Institut fur Normung (DIN) abrader as per DIN 53516.

Scanning electron microscopy (SEM) studies

The samples for SEM studies were cryogenically fractured and the surface was treated with osmium tetroxide (OsO_4) for 10 min to selectively stain the unsaturated SBR phase. These samples were sputter-coated with gold, and SEM examinations were performed on a Cambridge instrument (Canada) (S360). The morphology of the blend systems was also studied with an optical microscope (Leica Microsystem, Wetzer, Germany). For this, solutions of 5% SBR and EVA with varying proportions were prepared in chloroform. They were stirred for 36 h with a magnetic stirrer and then solution-cast as thin films 20 μm thick. Photomicrographs of the samples in the transmission mode with cross-polarized light and daylight filters were taken.

RESULTS AND DISCUSSION

Cure characteristics

Figure 1 shows the rheographs of the DCP-vulcanized SBR/EVA blends. The initial decrease in torque was due to the softening of the matrix. Torque then increased because of the formation of C—C crosslinks between the macromolecular chains. As shown in Figure 1, as the percentage of EVA increased in the blends, the rheometric torque decreased.

Table III shows the cure characteristics of the blends under investigation. The S-cured system exhibited the longest cure time and the mixed cured system exhibited the shortest cure time for a given blend ratio. In all of the systems, the cure time increased with increasing EVA content. *Scorch time* (t_2) is the time taken for the minimum torque value to increase by two units. It is a measure of the premature vulcanization of the material. It is clear from Table III that for a given vulcanizing system, as the EVA content increased, t_2 increased. This showed that the scorch safety of the blends increased with increasing EVA content. This was definitely associated with the saturated backbone of EVA. Among the different vulcanizing modes for a given blend, the scorch safety was highest for the S system and lowest for the DCP-cured system. The maximum torque, which is a measure of crosslink density, is also given in Table III.

RH, defined as the ratio between the torque and the time, was determined from the following relationship:

$$\mathrm{RH} = \frac{(M_{90} - M_2)}{(t_{90} - t_2)} \quad (1)$$

TABLE III
Cure Characteristics of the SBR/EVA Systems

Sample code	t_{90} (min)	M_{90} (dNm)	t_2 (min)	M_2 (dNm)	Maximum torque (dNm)	RH
S_0	20.5	5.47	8.5	0.75	6.08	0.39
S_{20}	23.2	3.51	9.3	0.42	3.90	0.22
S_{40}	24.3	2.67	10.9	0.29	2.97	0.18
S_{50}	24.7	1.97	12.7	0.25	2.19	0.14
S_{60}	27.6	1.61	13.0	0.25	1.79	0.09
S_{80}	29.9	0.57	16.0	0.20	0.63	0.03
P_0	16.7	9.58	1.3	0.72	10.65	0.57
P_{20}	17.8	8.61	1.5	0.49	9.57	0.49
P_{40}	18.0	7.20	2.0	0.37	8.00	0.43
P_{50}	18.5	6.67	2.1	0.33	7.4	0.39
P_{60}	19.0	6.07	2.2	0.31	6.74	0.34
P_{80}	19.5	5.07	2.5	0.22	5.64	0.29
P_{100}	19.9	4.18	2.9	0.19	4.65	0.23
M_0	7.5	6.74	2.2	0.67	7.49	1.15
M_{20}	12.2	4.46	3.9	0.46	4.96	0.48
M_{40}	12.9	4.61	5.2	0.36	4.01	0.42
M_{50}	13.5	2.33	6.5	0.36	2.59	0.28
M_{60}	15.8	2.49	7.3	0.32	2.77	0.26
M_{80}	19.0	1.69	12.0	0.23	1.88	0.21

where M_{90} corresponds to 90% of the maximum torque, M_2 is the minimum torque, t_{90} is the time required to achieve 90% of the maximum torque (optimum cure time), and t_2 is the scorch time. The calculated values of RH are also given in Table III. Interestingly, the RH decreased with increasing EVA content for all of the vulcanizing systems. This clearly indicated that SBR was the cure-activating component in the SBR/EVA blends.

Figure 2 shows the rheographs of the 50/50 SBR/EVA blends with different crosslinking systems. The DCP system exhibited the maximum torque, and the S system exhibited the lowest torque. This was because, unlike the S and mixed cured systems, DCP could cure both the SBR and EVA phases uniformly. Moreover, the rigid C—C crosslinked structure in the DCP system offered more resistance to the rheometric torque. A schematic representation of different crosslinks formed between the macromolecular chains during different vulcanization techniques is given in Figure 3.

Morphology

The properties of heterogeneous polymer blends are strongly dependent on the morphology of their systems. Several researchers[18–21] have related the variations in blend properties with the blend morphology. The optical micrographs of solution-cast, uncrosslinked SBR/EVA blends, as presented in Figure 4, showed that the system was immiscible. It is also shown that below 40 wt % EVA, the dispersed phase was EVA, and above 60% EVA, SBR was the dispersed phase in the blends.

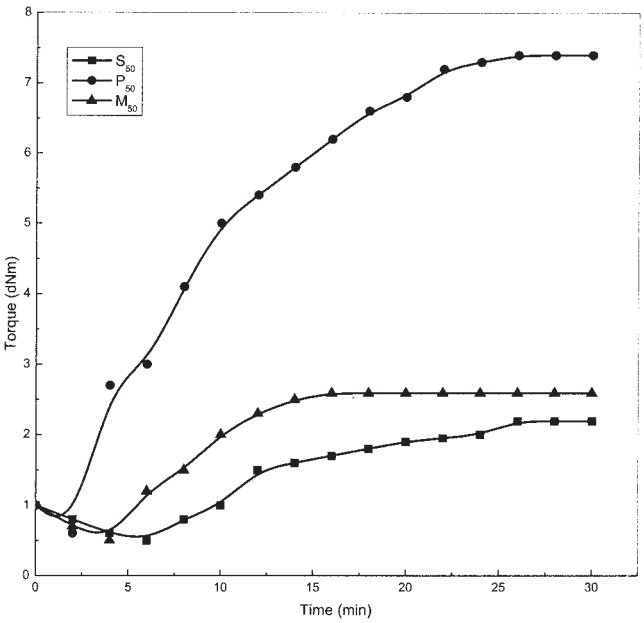

Figure 2 Rheographs of different crosslinked 50/50 SBR/EVA blends.

The scanning electron micrographs of the crosslinked SBR/EVA blends are presented in Figure 5. The gray region corresponds to SBR phase, which was stained by

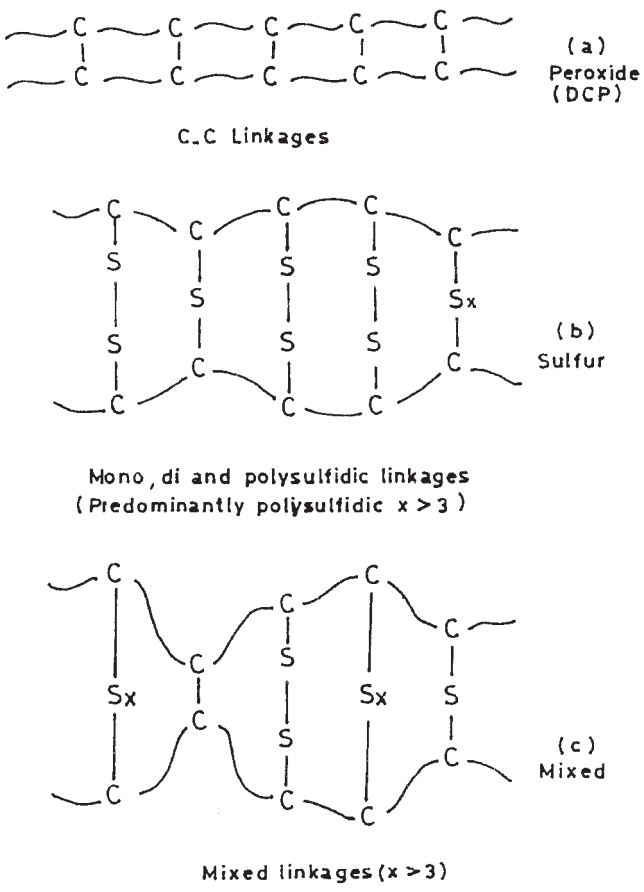

Figure 3 Schematic representation of the nature of the crosslinks.

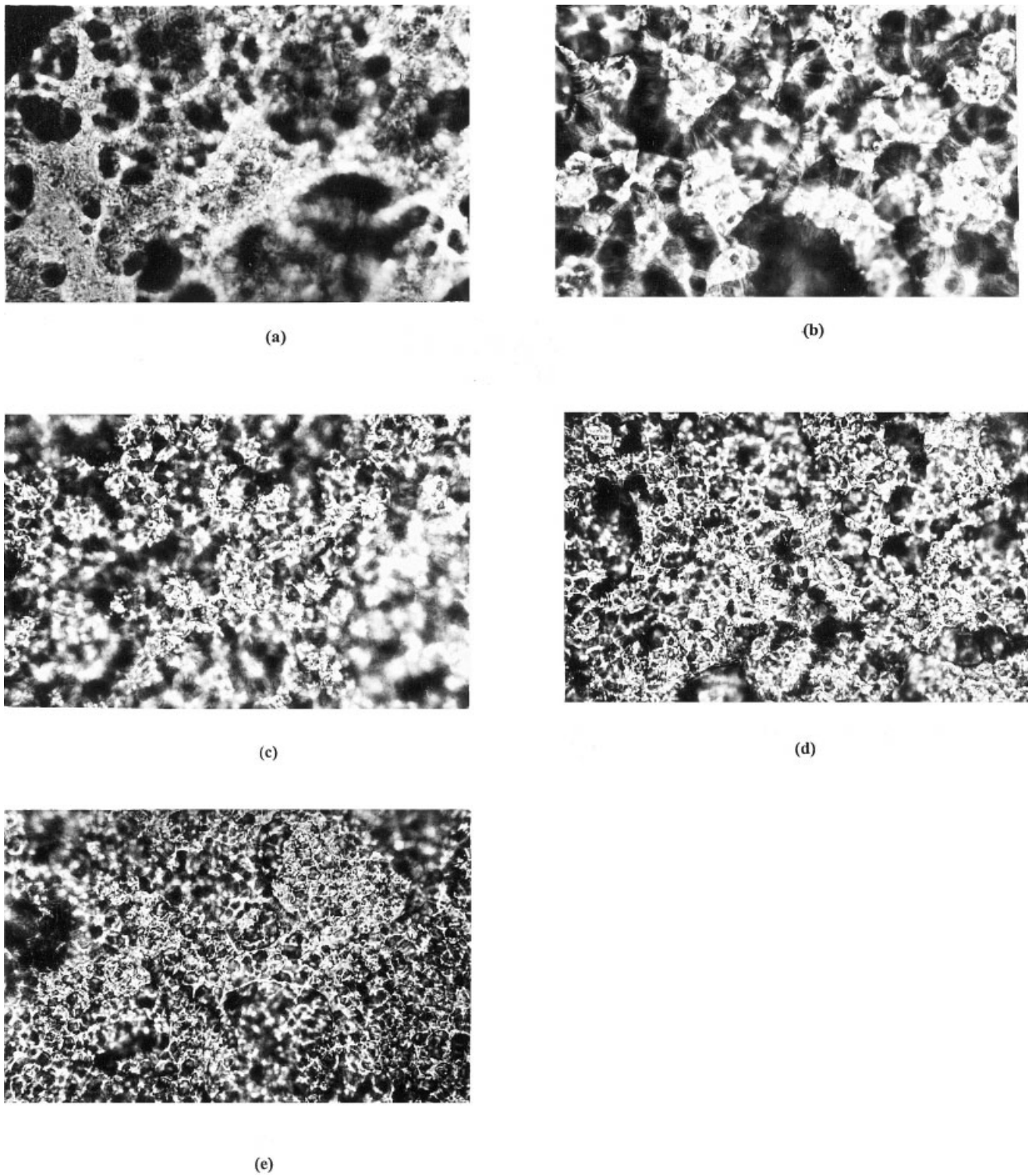

Figure 4 Optical micrographs showing the morphology of (a) 80/20 SBR/EVA, (b) 60/40 SBR/EVA, (c) 50/50 SBR/EVA, (d) 40/60 SBR/EVA, and (e) 20/80 SBR/EVA.

OsO_4, and the dark regions belong to the unstained EVA phase. Figure 5(a) shows the SEM photograph of the S_{40} blend system, where EVA was found to be dispersed as domains in the continuous SBR phase. Figure 5(b,c) shows the transformation of morphology with the incorporation of 60 and 80 wt % of EVA, respectively, into the SBR matrix. With increasing EVA content in the matrix, the domain size of the dispersed phase decreased, and a more continuous morphology was attained. This was also supported by optical micrographs, as shown in Fig-

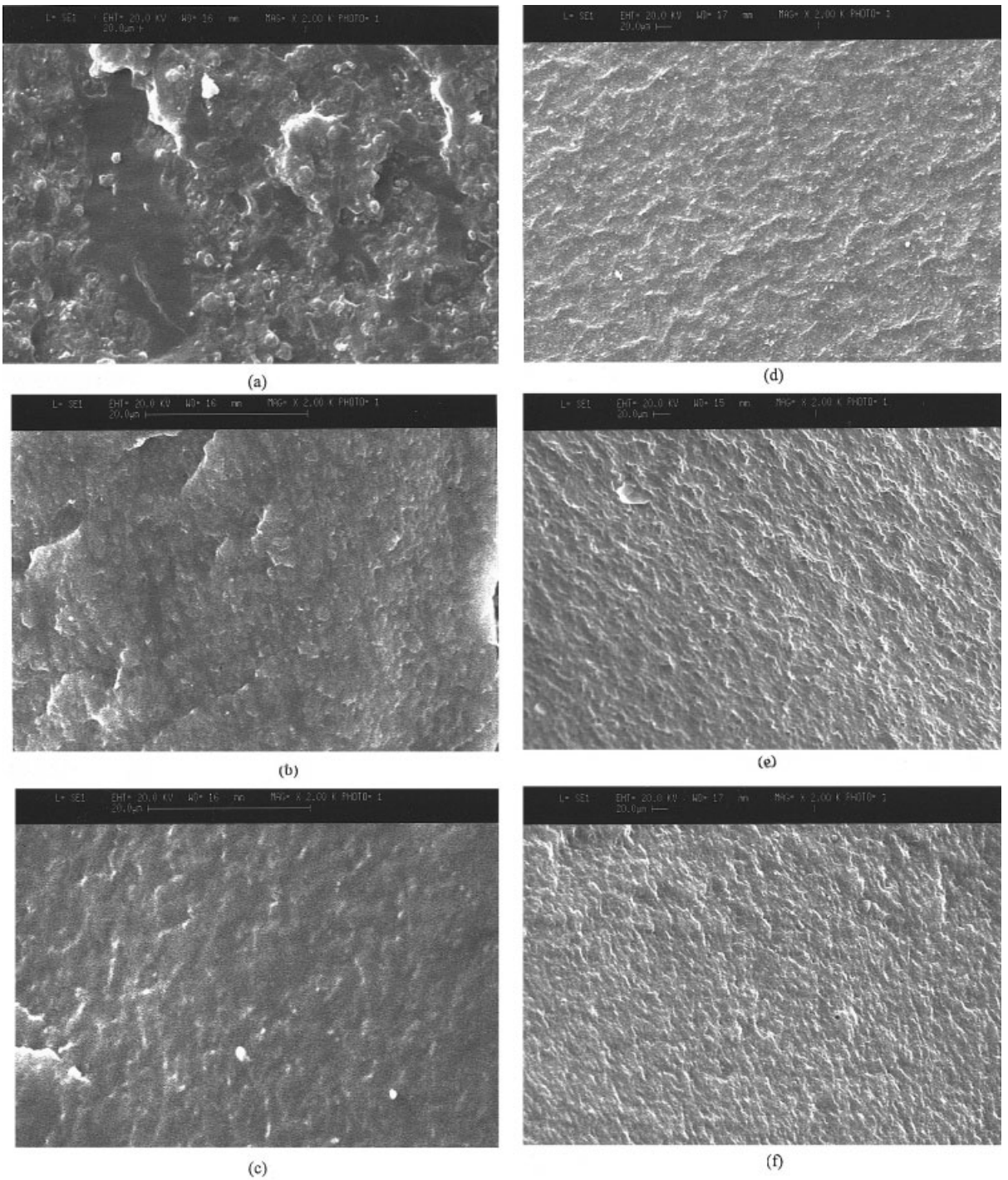

Figure 5 Scanning electron micrographs of (a) S_{40}, (b) S_{60}, (c) S_{80}, (d) P_{60}, (e) P_{80}, and (f) M_{60}.

ure 4. For the S_{80} system, a relatively cocontinuous morphology was observed. Figure 5(b,d,f) shows a comparison between the morphology of the S_{60}, P_{60}, and M_{60} systems. It is clear from the photographs that a fine and more uniform phase distribution was exhibited by the DCP-vulcanized sample. The domain size of the dispersed phase decreased in the order S > mixed > DCP vulcanizing systems for a given blend ratio. Figure 5(d,e) shows the comparison of the morphology of the P_{60} and P_{80} systems. There was a slight increase in EVA domain with increasing EVA content because of coalescence.

Effect of the blend ratio and curing systems on the mechanical properties

The nature of the deformation of the blends under an applied load can be understood from the stress–strain curves. The stress–strain curves of the peroxide-cured

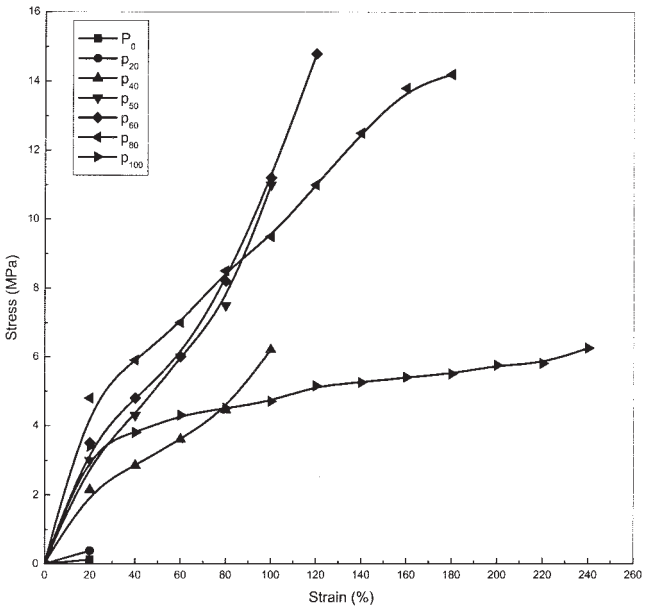

Figure 6 Effect of the blend ratio on the stress–strain curve of the DCP-cured SBR/EVA blends.

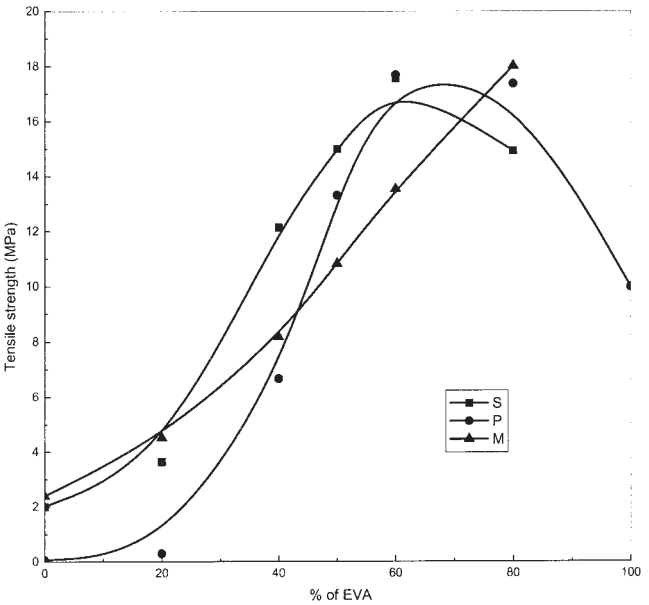

Figure 8 Effect of the blend ratio and different crosslinking systems on the tensile strength of the SBR/EVA blends.

system as a function of blend ratio are given in Figure 6. As shown, the deformation characteristics of these blends under an applied load increased with increasing EVA content in the blend. There was also an increase in the initial modulus with increasing EVA content in the blends. Thus, pure SBR (P_0) showed the lowest modulus and failed at fairly low stresses. As the EVA content in the blends increased, there was an increase in stress with increasing strain. This was due to the fact that under an applied load, the crystalline regions of EVA underwent rearrangement to accommodate more stress, while exhibiting higher elongation. Interestingly, the P_{50}, P_{60}, and P_{80} samples typically exhibited synergistic behavior. This clearly pointed toward better interaction between the components for these compositions.

The effects of different crosslinking systems on the stress–strain behavior of the SBR/EVA blend systems are given in Figure 7. The S and mixed systems showed almost similar stress–strain behavior and the

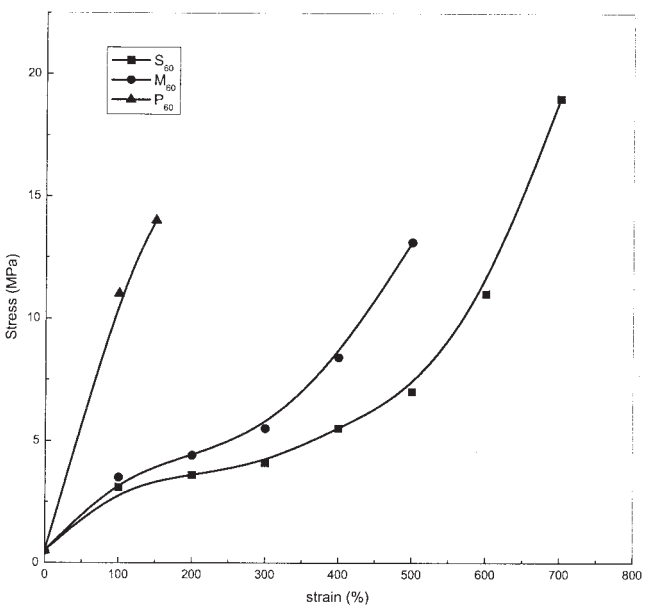

Figure 7 Effect of different curing systems on the stress–strain behavior of the SBR/EVA blends.

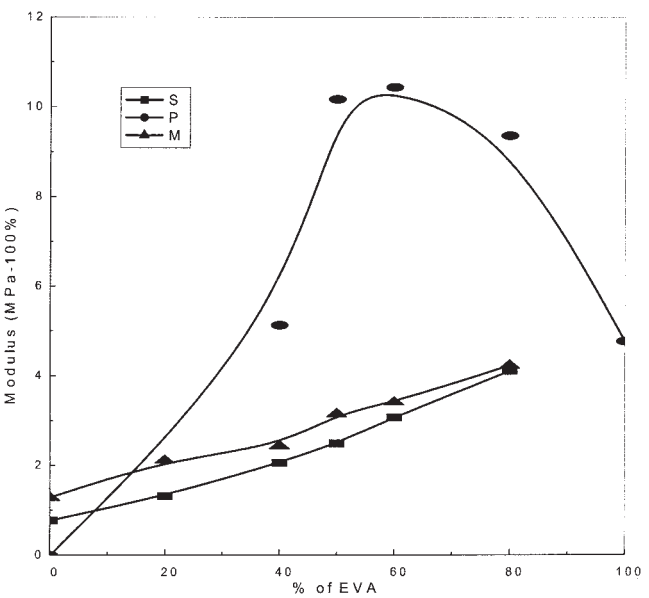

Figure 9 Effect of the blend ratio and different crosslinking systems on the modulus of the SBR/EVA blends.

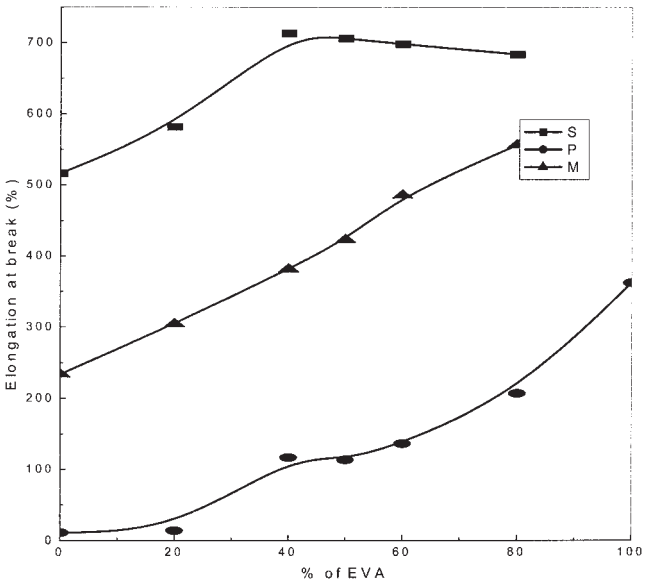

Figure 10 Effect of the blend ratio and different crosslinking systems on the elongation at break of the SBR/EVA blends.

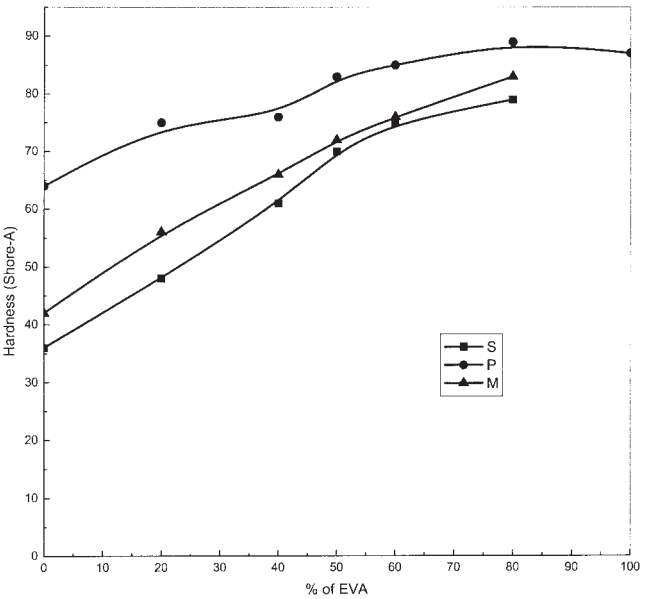

Figure 12 Effect of the blend ratio and different crosslinking systems on the hardness of the SBR/EVA blends.

initial modulus values were closer to each other. However, for the peroxide-cured system, the initial modulus was very high. This was probably because of the rigid C—C network in them. The bond lengths for the C—C, C—S, and S—S linkages were 1.54, 1.81, and 1.88 A°, respectively. Under an applied stress, the rigid C—C linkages did not yield and broke easily compared to the flexible C—S and S—S linkages. The highly flexible and labile S—S linkages were capable of withstanding higher stresses.

Figure 8 shows the variation of the tensile strengths of the blends with the blend ratio and different crosslinking systems. As shown, the EVA content in the blends increased as the tensile strength increased. The maximum tensile strength was observed in the blends with 60–80% EVA. As also shown in Figure 8, in the S-cured system; there was a drop in the tensile strength beyond 60% EVA. This was due to the phase inversion of the systems, as observed in the SEM photographs given in Figure 5(a–c). Beyond 60% EVA,

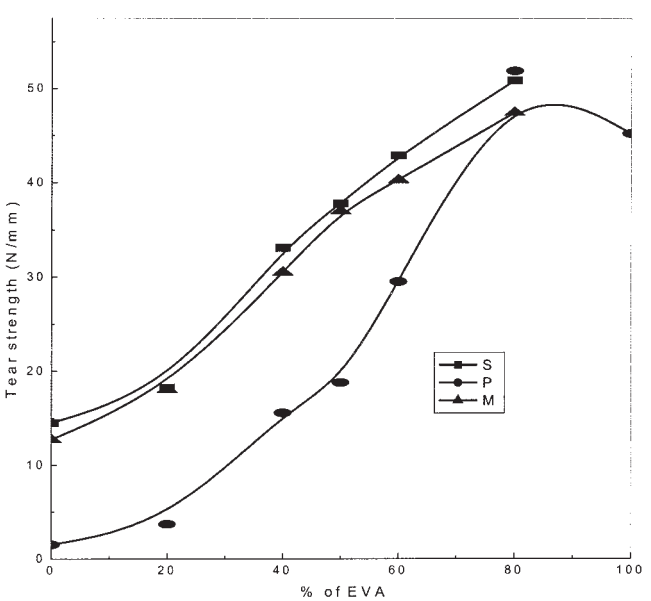

Figure 11 Effect of the blend ratio and different crosslinking systems on the tear strength of the SBR/EVA blends.

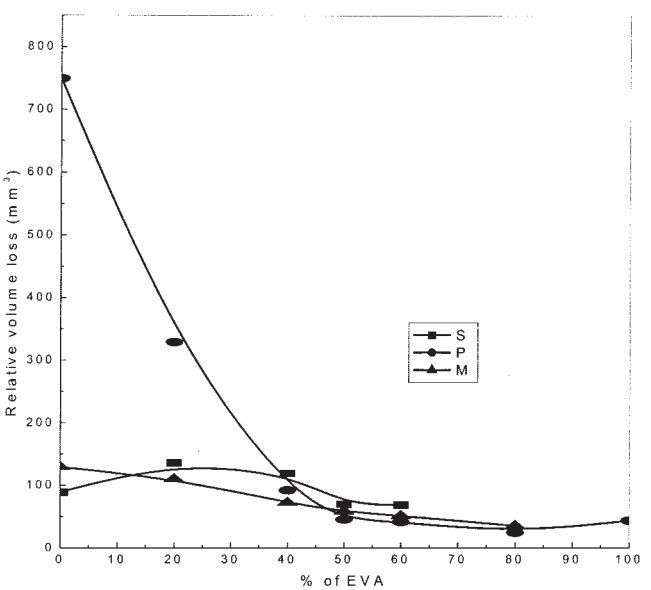

Figure 13 Effect of the blend ratio and different crosslinking systems on the relative volume loss of the SBR/EVA blends.

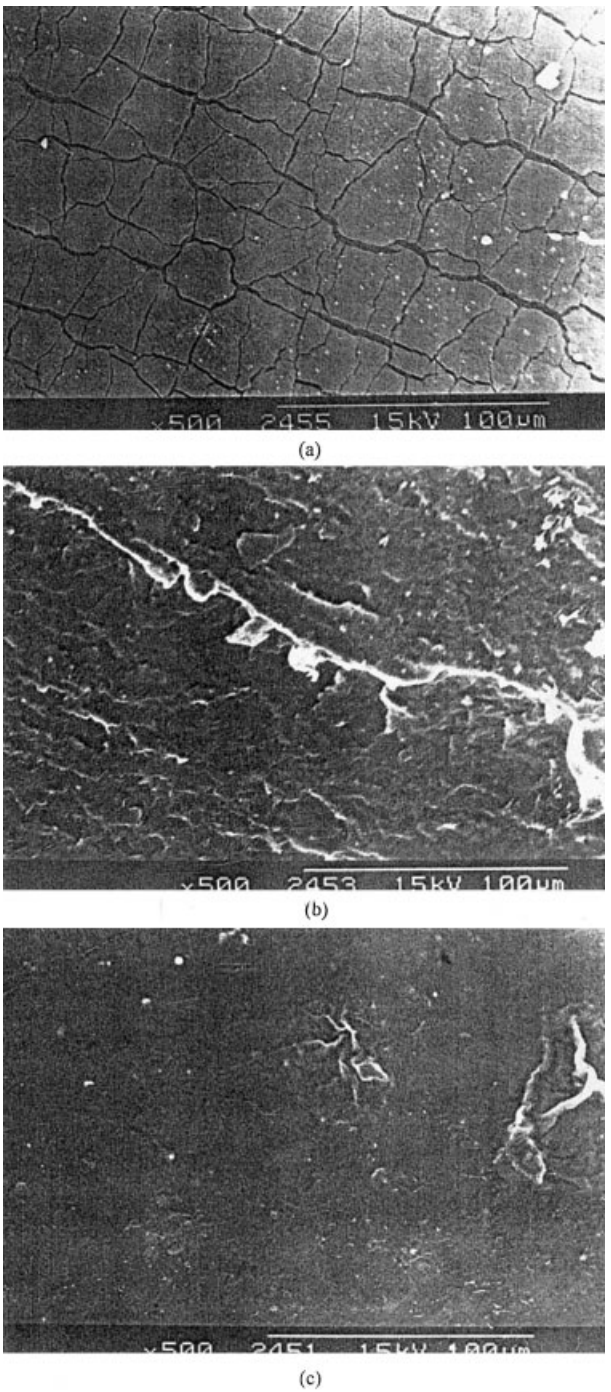

Figure 14 Scanning electron micrographs showing the tensile fracture surfaces of (a) P_{100}, (b) P_{50}, and (c) P_0.

EVA was the continuous phase, which could not be crosslinked by S. Thus, in the EVA-rich blends, the continuous phase remained uncrosslinked when S was the curing agent, and hence, a drop in the tensile strength beyond 60% EVA was observed. For the peroxide-cured system, there was a drop in the tensile strength beyond 60% EVA. This was due to the increase in the domain size of the dispersed SBR phase due to the coalescence, as shown in Figure 5(d,e).

Figure 9 shows the variation in the modulus of the blends crosslinked with the three different curing systems with weight percentage of EVA. As shown, in the S and mixed systems, the modulus increased with increasing EVA content up to 80%, whereas the DCP system showed an increase in the modulus up to 60% EVA and then decreased. The decrease in modulus beyond 60% EVA content in the DCP system was probably due to the decrease in adhesion at the interface, which resulted in coalescence and an increased domain size.

Figure 10 shows the variation in elongation at break with weight percentage of EVA for the systems with different crosslinking systems. For all three vulcanizing systems, the elongation at break increased with increasing EVA content. This was due to the orientation of the crystalline regions of EVA in the direction of elongation. Also, the DCP cured system showed lower elongation at break compared to the other cure systems. This was attributed to the C—C crosslinks between the macromolecular chains in the DCP system.

Figure 11 shows the variation in tear strength with blend ratio and crosslinking systems. The tear strength of all three systems increased with increasing EVA content because of the increase in interfacial adhesion between the two components. The tear strength was at a maximum for blends with 80% EVA for all of the crosslinking systems. This was supported by the SEM photographs presented earlier. Also, the DCP system showed a lower tear strength compared to the S-cured and mixed-cured systems. This was also due to the short and rigid C—C bonds present in the DCP cured system.

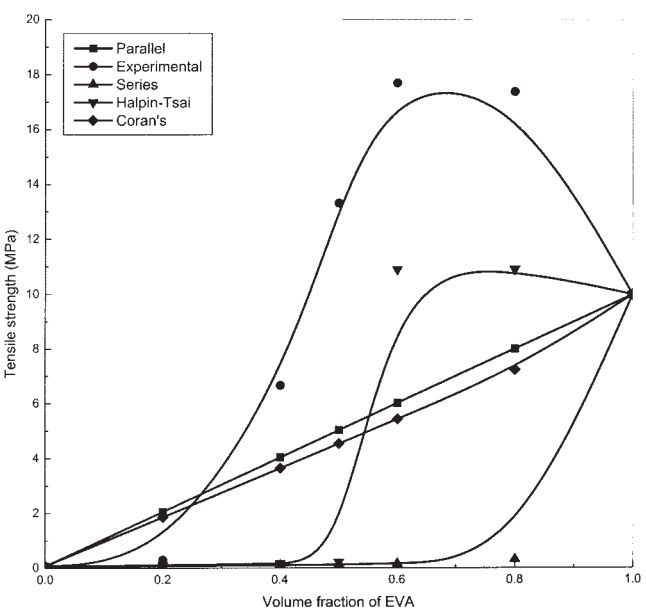

Figure 15 Applicability of various models on the tensile strength of the DCP-cured SBR/EVA blends.

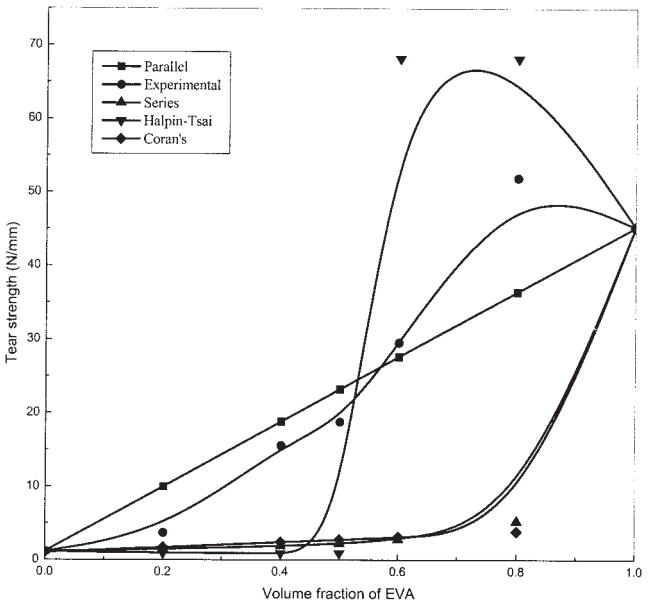

Figure 16 Applicability of various models on the tear strength of the DCP-cured SBR/EVA blends.

Figure 12 shows the variation in hardness with the weight percentage of EVA for the blends with different crosslinking systems. For all three systems, the hardness increased with increasing EVA content. Among the three systems, the DCP system showed the highest hardness.

Figure 13 shows the variation in relative volume loss with the weight percentage of EVA and the nature of crosslinks in these blend systems. In the DCP and mixed systems, the relative volume loss decreased with increasing EVA content. The significant relative volume loss observed for the DCP system could have been due to its short and rigid C—C crosslinks. For the S-cured system, the relative volume loss increased up to 40% EVA content and then decreased.

Fracture surface morphology

SEM has been successfully used by several researchers to follow the failure mechanism in polymer blends.[22–26] The scanning electron micrographs of the tensile fracture surfaces of the P_{100}, P_{50}, and P_0 samples are shown in Figure 14(a–c). P_{100} showed a fracture surface full of cracks, which was due to the semicrystalline nature of EVA. P_{50} showed a ductile failure with a rough surface, and P_0 exhibited a smooth failure surface, which is characteristic for rubbers.

Model fitting

Mechanical properties are widely suited for the analysis of multicomponent systems through a comparison of experimental results and predictions based on various models. The application of various composite models gives a broader insight into the properties of blends. It also helps one to check assumptions regarding the structure, mechanism, and properties of the interface. Several theories have been proposed to predict tensile properties in terms of various parameters. The different models selected to predict the mechanical behavior of this blend system included the parallel model, series model, Halpin–Tsai equation, and Coran's equation.

The parallel model (highest upper bound model) is given by the following equation:[27]

$$M = M_1\phi_1 + M_2\phi_2 \tag{2}$$

where M is the mechanical property of the blend and M_1 and M_2 are the mechanical properties of components 1 and 2,respectively, and ϕ_1 and ϕ_2 are the volume fractions of components 1 and 2, respectively. In this model, the components are considered to be arranged parallel to one another so that the applied stress elongates each of the components by the same amount.

In the lowest lower bound series model, the components are arranged in series with the applied stress. The equation[27] is

$$1/M = \phi_1/M_1 + \phi_2/M_2 \tag{3}$$

According to the Halpin–Tsai equation[28]

$$M_1/M = (1 + A_iB_i\phi_2)/(1 - B_i\phi_2) \tag{4}$$

where

$$B_i = (M_1/M_2 - 1)/(M_1/M_2 + A_i) \tag{5}$$

In these equations, subscripts 1 and 2 refer to the continuous and dispersed phase, respectively. The constant A_i is defined by the morphology of the system. $A_i = 0.66$ when a flexible component forms the dispersed phase in a continuous hard matrix. However, if the hard material forms the dispersed phase in a continuous flexible matrix, $A_i = 1.5$.

In Coran's model, the mechanical properties are generally between the parallel model upper bound (M_U) and the series model lower bound (M_L).

According to Coran's equation[29]

$$M = f(M_U - M_L) + M_L \tag{6}$$

where f varies between 0 and 1. The value of f is a function of phase morphology and is given by

$$f = V_H^n(nV_s + 1) \tag{7}$$

where n is related to phase morphology and V_H and V_S are the volume fractions of the hard and soft phases, respectively.

Figures 15 and 16 show the comparisons between the experimental and theoretical curves for the tensile and tear strengths of the SBR/EVA blends. For the tensile strength, the experimental values were higher at higher proportions of EVA compared to the theoretical predictions. There was only a marginal increase in the tensile strength with the addition of up to 20 wt % EVA to SBR. A very large increase in the tensile strength was observed when 20–60 wt % of EVA was added to SBR. In immiscible blends, the tensile strength usually depends on the particle size of the dispersed phase.[30] The lower values for the tensile strength in this blend system up to 20 wt % EVA may have been due to the poor interfacial adhesion between the dispersed EVA and the continuous SBR matrix. The poor interfacial adhesion caused premature failure as a result of the usual crack-opening mechanism. The experimental values of the tear strength were close to the parallel model with a negative deviation at a lower volume fraction of EVA and then a positive deviation at a higher EVA content.

CONCLUSIONS

The curing behavior, morphology, mechanical properties, and failure mode of SBR/EVA blends were studied with special reference to the effects of the blend ratio and crosslinking systems. From the cure characteristics, we observed that the mixed cure system showed the shortest cure time. Better scorch safety was exhibited by the S-cured system. In EVA-rich blends, there was an increase in stress with an increase in strain, which was due to the orientation of crystalline regions of EVA in the direction of stress. The differences in the stress–strain behavior of blends with different crosslinking systems were explained on the basis of the nature of the crosslinks formed during vulcanization. A relatively cocontinuous morphology was observed for 20/80 SBR/EVA blends with better properties. The tensile failure surfaces were observed under a scanning electron microscope to follow the failure mechanism. The P_{100} sample exhibited a cracked tensile fracture surface due to its crystallinity, and P_0 exhibited a smooth fracture surface, which is characteristic for rubbers. The applicability of various theoretical models to predict the properties of the blends was also checked. For the tensile strength, experimental values were higher than the theoretically predicted ones at higher proportions of EVA. For tear strength, the experimental values were closer to the parallel model with a positive deviation at higher percentages of EVA.

References

1. Ismail, H.; Nizam, J. M.; Abdul Khalil, H. P. S. Int J Polym Mater 2001, 48, 461.
2. Okwu, U. N.; Okieimen, F. E. Eur Polym J 2001, 37, 2253.
3. Shinski, A. J.; Keskkula, H.; Paul, D. R. Polymer 1992, 33, 284.
4. Ismail, H.; Suzaimah, S. Polym Plast Technol Eng 2000, 39, 817.
5. Mohammed, M. G.; Abd-El-Messieh, S. L.; El-Sabbagh, S.; Younan, A. P. J Appl Polym Sci 1998, 69, 775.
6. Nelson, P. A.; Kutty, S. K. N. Polym Plast Technol Eng 2004, 43, 245.
7. Amraee, I. A.; Katbab, A. A.; Aghafarajollah, S. Rubber Chem Technol 1996, 69, 130.
8. Ismail, H.; Suzaimah, S. Polym Test 2000, 19, 879.
9. Ghilarducci, A.; Cerveny, S.; Salva, H.; Matteo, C. L.; Marzocca, A. J. Kautsch Gummi Kunstst 2001, 54, 382.
10. Varghese, H.; Bhagawan, S. S.; Thomas, S. J Appl Polym Sci 1999, 71, 2335.
11. Mishra, S.; Baweja, B.; Chandra, R. J Appl Polym Sci 1999, 74, 2756.
12. Yoon, J.-S.; Oh, S.-H.; Kim, M.-N.; Chin, I.-J.; Kim, Y.-H. Polymer 1999, 40, 2303.
13. Kundu, P. P.; Tripathy, D. K. Kautsch Gummi Kunstst 1996, 49, 268.
14. Kundu, P. P.; Tripathy, D. K.; Gupta, B. R. J Appl Polym Sci 1997, 63, 187.
15. Koshy, A. T.; Kuriakose, B.; Thomas, S.; Premalatha, C. K.; Varghese, S. J Appl Polym Sci 1993, 49, 901.
16. Koshy, A. T.; Kuriakose, B.; Thomas, S.; Varghese, S. Polymer 1993, 34, 3428.
17. Binet, S. M. J Polym Eng 1993, 12, 121.
18. Cimmino, S.; Dorazio, L.; Greco, R.; Maglio, G.; Malinconico, M.; Mancarella, C.; Martuscelli, E.; Palumbo, R.; Ragosta, G. Polym Eng Sci 1984, 24, 48.
19. Greco, R.; Mancarella, C.; Martuscelli, E.; Ragosta, G.; Jinghua, Y. Polymer 1987, 28, 1929.
20. Choi, G. D.; Kim, S. H.; Jo, W. H. Polymer 1996, 28, 527.
21. Bagheri, R.; Pearson, R. A. J Mater Sci 1996, 31, 3945.
22. Gent, A. N.; Pulford, C. T. R. J Mater Sci 1984, 19, 3612.
23. Kuriakose, B.; De, S. K. J Mater Sci 1985, 20, 1864.
24. Bhagawan, S. S.; Tripathy, D. K.; De, S. K. J Mater Sci 1987, 6, 157.
25. Thomas, S.; Kuriakose, B.; Gupta, B. R.; De, S. K. J Mater Sci 1986, 21, 711.
26. Thomas, S.; Gupta, B. R.; De, S. K. J Vinyl Technol 1987, 9, 71.
27. Thomas, S.; George, A. Eur Polym J 1992, 28, 1451.
28. Nielson, L. E. Rheol Acta 1974, 13, 86.
29. Coran, A. Y. Hand Book of Elastomers, New Developments, Technology; Bhowmick, A. K.; Stephens, H. L., Eds.; Marcel Dekker: New York, 1998; p 249.
30. Joseph, S.; Thomas, S. J Polym Sci Part B: Polym Phys 2002, 40, 755.